Original Article

Novel Mutation in the α-Myosin Heavy Chain Gene Is Associated With Sick Sinus Syndrome

Taisuke Ishikawa, DVM, PhD; Chuanchau J. Jou, DO, PhD; Akihiko Nogami, MD, PhD; Shinya Kowase, MD; Cammon B. Arrington, MD, PhD; Spencer M. Barnett, BS; Daniel T. Harrell, BS; Takuro Arimura, DVM, PhD; Yukiomi Tsuji, MD, PhD; Akinori Kimura, MD, PhD; Naomasa Makita, MD, PhD

Background—Recent genome-wide association studies have demonstrated an association between *MYH6*, the gene encoding α-myosin heavy chain (α-MHC), and sinus node function in the general population. Moreover, a rare *MYH6* variant, R721W, predisposing susceptibility to sick sinus syndrome has been identified. However, the existence of disease-causing *MYH6* mutations for familial sick sinus syndrome and their underlying mechanisms remain unknown.

Methods and Results—We screened 9 genotype-negative probands with sick sinus syndrome families for mutations in *MYH6* and identified an in-frame 3-bp deletion predicted to delete one residue (delE933) at the highly conserved coiled-coil structure within the binding motif to myosin-binding protein C in one patient. Co-immunoprecipitation analysis revealed enhanced binding of delE933 α-MHC to myosin-binding protein C. Irregular fluorescent speckles retained in the cytoplasm with substantially disrupted sarcomere striation were observed in neonatal rat cardiomyocytes transfected with α-MHC mutants carrying delE933 or R721W. In addition to the sarcomere impairments, delE933 α-MHC exhibited electrophysiological abnormalities both in vitro and in vivo. The atrial cardiomyocyte cell line HL-1 stably expressing delE933 α-MHC showed a significantly slower conduction velocity on multielectrode array than those of wild-type α-MHC or control plasmid transfected cells. Furthermore, targeted morpholino knockdown of *MYH6* in zebrafish significantly reduced the heart rate, which was rescued by coexpressed wild-type human α-MHC but not by delE933 α-MHC.

Conclusions—The novel *MYH6* mutation delE933 causes both structural damage of the sarcomere and functional impairments on atrial action propagation. This report reinforces the relevance of *MYH6* for sinus node function and identifies a novel pathophysiology underlying familial sick sinus syndrome. **(*Circ Arrhythm Electrophysiol*. 2015;8:400-408. DOI: 10.1161/CIRCEP.114.002534.)**

Key words: genetics ■ MYH6 ■ myosin heavy chain ■ sick sinus syndrome ■ sinus node dysfunction

Sick sinus syndrome (SSS) is a common arrhythmia often associated with aging, structural heart diseases, or surgical injury, but can also occur in a familial form.[1] Several studies have demonstrated genetic mutations in both sporadic and familial cases of SSS.[2–4] Affected ion channel or ion channel–associated genes identified to date include sodium channel, Nav1.5 (*SCN5A*),[2] ankyrin-B (*ANK2*),[3] and hyperpolarization-activated channel (*HCN4*).[4] Mutations in *HCN4* result in sinus node dysfunction caused by a reduction of the pacemaker current, whereas *SCN5A* mutations lead to conduction delay within the sinus node or exit block.[5]

MYH6 and *MYH7* encode the homologous myosin heavy chain (MHC) isoforms α-MHC and β-MHC, respectively, in cardiomyocytes, which play pivotal roles in the organization of sarcomeric structures and muscle contraction.[6–8] *MYH7* is predominantly expressed in the adult ventricle, whereas *MYH6* is mainly expressed in the fetal heart and adult atrium.[9] *MYH7* is a well-established causative gene with over 300 mutations responsible for hypertrophic cardiomyopathy and dilated cardiomyopathy,[10,11] whereas more limited *MYH6* mutations have been reported in cardiomyopathy[12,13] and congenital heart disease, such as atrial septal defect.[7,14–17] On the contrary, recent genome-wide association studies demonstrated that a common nonsynonymous variant A1101V in *MYH6* was associated with an increased resting heart rate,[17–19] whereas another rare nonsynonymous variant (resulting in R721W) was associated with a high risk of SSS.[20]

Received November 12, 2014; accepted February 11, 2015.

From the Department of Molecular Physiology, Nagasaki University Graduate School of Biomedical Sciences, Nagasaki (T.I., D.T.H., Y.T., N.M.); Department of Molecular Pathogenesis, Medical Research Institute, Tokyo Medical and Dental University, Tokyo, Japan (T.I., T.A., A.K.); Division of Pediatric Cardiology, University of Utah, Salt Lake City (C.J.J., C.B.A., S.M.B.); Cardiovascular Division, University of Tsukuba, Tsukuba (A.N.); Department of Heart Rhythm Management, Yokohama Rosai Hospital, Yokohama (A.N., S.K.); and Department of Veterinary Medicine, Kagoshima University, Kagoshima, Japan (T.A.).

The Data Supplement is available at http://circep.ahajournals.org/lookup/suppl/doi:10.1161/CIRCEP.114.002534/-/DC1.

Correspondence to Naomasa Makita, MD, PhD, Department of Molecular Physiology, Nagasaki University, Graduate School of Biomedical Sciences, 1-12-4 Sakamoto, Nagasaki 852–8523, Japan, E-mail makitan@nagasaki-u.ac.jp or Akinori Kimura, MD, PhD, Department of Molecular Pathogenesis, Medical Research Institute, Tokyo Medical and Dental University, 1-5-45 Yushima, Bunkyo-ku, Tokyo 113–8510, Japan, E-mail akitis@mri.tmd.ac.jp

WHAT IS KNOWN

- Sick sinus syndrome (SSS) is often associated with aging and structural heart diseases, but it may occur in a familial form.
- Recent genome-wide association studies uncovered MYH6 encoding atrial myosin heavy chain as a susceptibility gene for heart rate and SSS; however, its underlying mechanisms and the existence of causative mutations for SSS remain unknown.
- Here, we report a novel *MYH6* mutation delE933 in an SSS patient who has a family history of SSS.

WHAT THE STUDY ADDS

- When expressed in cardiomyocytes, delE933-*MYH6* impaired the atrial action potential propagation and disrupted sarcomere integrity consistent with the R721W-*MYH6*, a high risk genetic predisposition for SSS demonstrated in Icelanders.
- Our data reinforces the relevance of *MYH6* of sinus node function and suggested that structural damages of the sarcomere and functional impairments on atrial action potential propagation may underlie familial SSS with *MYH6* mutations.

Moreover, heterozygous zebrafish carrying the *MYH6* mutation N695K (*MYH6*$^{hu/423/+}$) displayed partial atrial contractile defects.[21] Based on these observations, it is conceivable that some *MYH6* variations impair the sarcomere structure and function of the atrium, which in turn would cause electrophysiological abnormalities and sinus node dysfunction. However, it remains to be elucidated whether (1) *MYH6* is the causative gene for familial SSS and (2) the genetic variations of *MYH6* associated with SSS confer pacemaker dysfunction through structural damage of the sarcomere of the atrial muscle surrounding the sinus node or by functional impairment of the pacemaker channel or sodium channel. The present study identified a novel *MYH6* mutation in one SSS proband and investigated the means by which this could confer sinus node dysfunction.

Methods

Genetic Screening of *MYH6* Mutations

We previously performed genetic screening of mutations in *SCN5A* and *HCN4* in 15 probands afflicted with familial SSS and found 6 distinct *SCN5A* mutations.[22] In this study, we enrolled 9 SSS families out of this cohort, which were free from *SCN5A* or *HCN4* mutations. Age at diagnosis of the probands (3 male and 6 female) ranged from 3 to 65 years old (44.6±21.8 years old; mean±SD).

Genomic DNA was extracted from peripheral blood of each subject using standard methods. Coding regions of *MYH6* were amplified by polymerase chain reaction using exon-flanking intronic primers (Table I in the Data Supplement). Direct DNA sequencing was performed using ABI 3130 genetic analyzers (Life Technologies, Carlsbad, CA). Mutations were validated by the analysis of unrelated 400 healthy Japanese individuals and dbSNP, 1000 Genome Project, Exome Variant Server, and Human Genetic Variation Database (HGVD, Japanese variation database, http://www.genome.med.kyoto-u.ac.jp/SnpDB/). All probands and family members who participated in the study gave their written informed consent in accordance with the Declaration of Helsinki. The research protocol was approved by the Ethics Review Committee of Nagasaki University and the Ethics Review Committee of Medical Research Institute, Tokyo Medical and Dental University.

Alignment of Amino Acid Sequences and Structural Prediction of α-MHC

Amino acid sequence of human α-MHC was aligned using the HomoloGene program with those of other species, and the phylogenetic conservations were testified among human MHC isoforms (the GenBank accession number of each gene is listed in Tables II and III in the Data Supplement). Alterations of the coiled-coil structure of the α-MHC were predicted in silico by using SWISS-MODEL (http://swissmodel.expasy.org/) and visualized by a software RasTop (http://www.geneinfinity.org/rastop/).

Plasmids and cRNA preparation

A 5.8 kb cDNA fragment of human *MYH6* was obtained by reverse transcription-polymerase chain reaction from human heart RNA using a primer pair *MYH6*-F-EcoRV and *MYH6*-R-Sal1 (Table I in the Data Supplement) and was cloned into pEGFP-C1 (Takara Bio, Shiga, Japan) to make green fluorescent protein (GFP)-tagged *MYH6* plasmid (pEGFP-*MYH6*). Mutant *MYH6* plasmids of R721W (c.2161C>T) and delE933 (c.2797_2799delGAG) were constructed using an overlap-extension polymerase chain reaction strategy.

To assess the binding affinity of the mutant S2 region of α-MHC to myosin-binding protein C (MyBP-C) on the basis of the previous report,[8] cDNAs corresponding to the binding regions for human α-MHC (S2 region; aa. 884–965 of NP_002462) and human MyBP-C (C1C2 region; aa. 256–363 of NP_000247) were amplified and cloned into the c-myc-tag plasmid pCMV-Tag3B (Takara Bio; pCMV3B-*MYH6*-S2) and the pEGFP-C1 (pEGFP-*MYBPC3*-C1C2), respectively. All constructs were sequenced to ensure that no errors were introduced.

For the zebrafish experiments, wild-type (WT) and mutant *MYH6* cDNA fragments were, respectively, cloned into pIRES2-EGFP vector (Takara Bio; pIRES2-EGFP-*MYH6*) and pCS2+ vector[23] (pCS2-*MYH6*) by using specific primer pairs (Table I in the Data Supplement). cRNAs of human *MYH6* were synthesized using the mMessage mMachine in vitro transcription kit (Life Technologies) and purified as described previously.[24] Purified mutant cRNAs were sequenced by the University of Utah sequencing core facility.

Coimmunoprecipitation Assay

HeLa cells were cotransfected with pEGFP-*MYBPC3*-C1C2 and pCMV3B-*MYH6*-S2 using Transfectin lipid reagent (BioRad, Hercules, CA). After 48 hours of the transfection, cells were lysed in protein extraction buffer (1% Nonidet P-40, 1 mmol/L EDTA, 150 mmol/L NaCl, and 10 mmol/L Tris-HCl, pH 7.8) containing Protease Inhibitor Cocktail. Total cellular lysate was obtained by centrifugation at 13 000*g* for 5 minutes, and its protein concentration was measured by BCA (bicinchoninic acid) protein assay (Thermo Fisher Scientific, Waltham, MA). Coimmunoprecipitation assay was performed using equal amount of cellular lysate with goat anti-myc polyclonal antibody (Sigma-Aldrich, St. Louis, MO) using the Catch and Release version 2.0 reversible immunoprecipitation system (Millipore, Billerica, MA). Immunoprecipitates were separated on a 9% SDS-polyacrylamide gel and transferred to a nitrocellulose membrane. After blocking with 5% skim milk in PBS, membranes were incubated with primary anti-GFP monoclonal antibody (1:100, Santa Cruz Biotechnology, Dallas, TX) overnight at 4°C and rabbit-anti mouse IgG horseradish peroxidase (HRP)–conjugated antibody (Dako, Grostrup, Denmark) for 1 hour at RT. Signals were visualized by Immobilon Western Chemiluminescent HRP Substrate (Millipore) and Luminescent Image Analyzer LAS-3000 mini (Fujifilm, Tokyo, Japan).

Immunofluorescence Study

Immunohistological study was performed using neonatal rat ventricular cardiomyocytes prepared from 1-day-old Sprague–Dawley rats as described previously.[25] Briefly, neonatal rat ventricular cardiomyocytes (4×10^4) were transfected with WT or mutant pEGFP-*MYH6* plasmid with Lipofectamine LTX. Twenty-four hours later, the cells were fixed with 100% ethanol, stained by primary mouse anti-α-actinin antibody (1:100, Sigma-Aldrich) overnight at 4°C and visualized with secondary Alexa Fluor 568 goat antimouse IgG antibody (1:500, Life Technologies). The fluorescent images were analyzed using LSM510 laser-scanning confocal microscope with a 63× oil immersion objective lens (Carl-Zeiss Microscopy, Jena, Germany).

All care and treatment of animals were in accordance with the guidelines for the Care and Use of Laboratory Animals published by the National Institute of Health (NIH Publication, eighth edition 2011) and subjected to prior approval by the animal protection authorities of Nagasaki University and Tokyo Medical and Dental University.

Action Potential Propagation Velocity Measurements in HL-1 Cells Stably Expressing Human *MYH6*

The mouse atrial cardiomyocyte cell line HL-1 (4×10^5), gift from Dr Claycomb, was cultured as previously described.[26] Cells were transfected with 2 μg of linearized pIRES2-EGFP-*MYH6* plasmids of WT or delE933 or pIRES2-EGFP plasmid and 4 μl of Lipofectamine LTX (Life Technologies) according to the manufacturer's instructions. Forty-eight hours after transfection, cells were cultured in the presence of 400 μg/mL G418 (Life Technologies) for 4 weeks to establish stable cell lines.

Stable HL-1 cells (1×10^5 cells) expressing WT-*MYH6*, delE933-*MYH6*, or mock pIRES2-EGFP were plated on 8×8 planner multielectrode arrays (array size 1 mm×1 mm; electrode diameter 50 μm; Alpha MED Scientific Inc., Osaka, Japan) precoated with gelatin and fibronectin (Sigma-Aldrich). Seventy-two hours later, a single stimulus of 10 μA was applied on a designated point to initiate spontaneous beating, and electric field potentials were recorded for 1 minute. Action potential propagation velocity was calculated by averaging the velocities between the stimulation point and the remaining 63 points. Cell numbers on the array were counted after recordings with detaching them from the arrays with Trypsin-EDTA. These procedures were repeated 4 times for each line.

In Vivo Evaluation of Overexpressed *MYH6* in Zebrafish

Transgenic zebrafish (cmlc2:GFP, *Danio rerio*) embryos were used to functionally characterize the zebrafish *myh6* and human *MYH6* variant. *MYH6* ATG-blocking morpholino antisense oligonucleotide (myh6 ATG-MO) was designed to target *myh6* (Table I in the Data Supplement).[27] Myh6 ATG-MO (0.5–1 ng/embryo) was injected alone or coinjected with WT or delE933 *MYH6* cRNA (0.4 ng/embryo) at the 1- to 2-cell stage. After the injection, embryos were maintained in embryo water at 28°C and staged according to age and morphological criteria.[28] Cardiac phenotypes were screened using

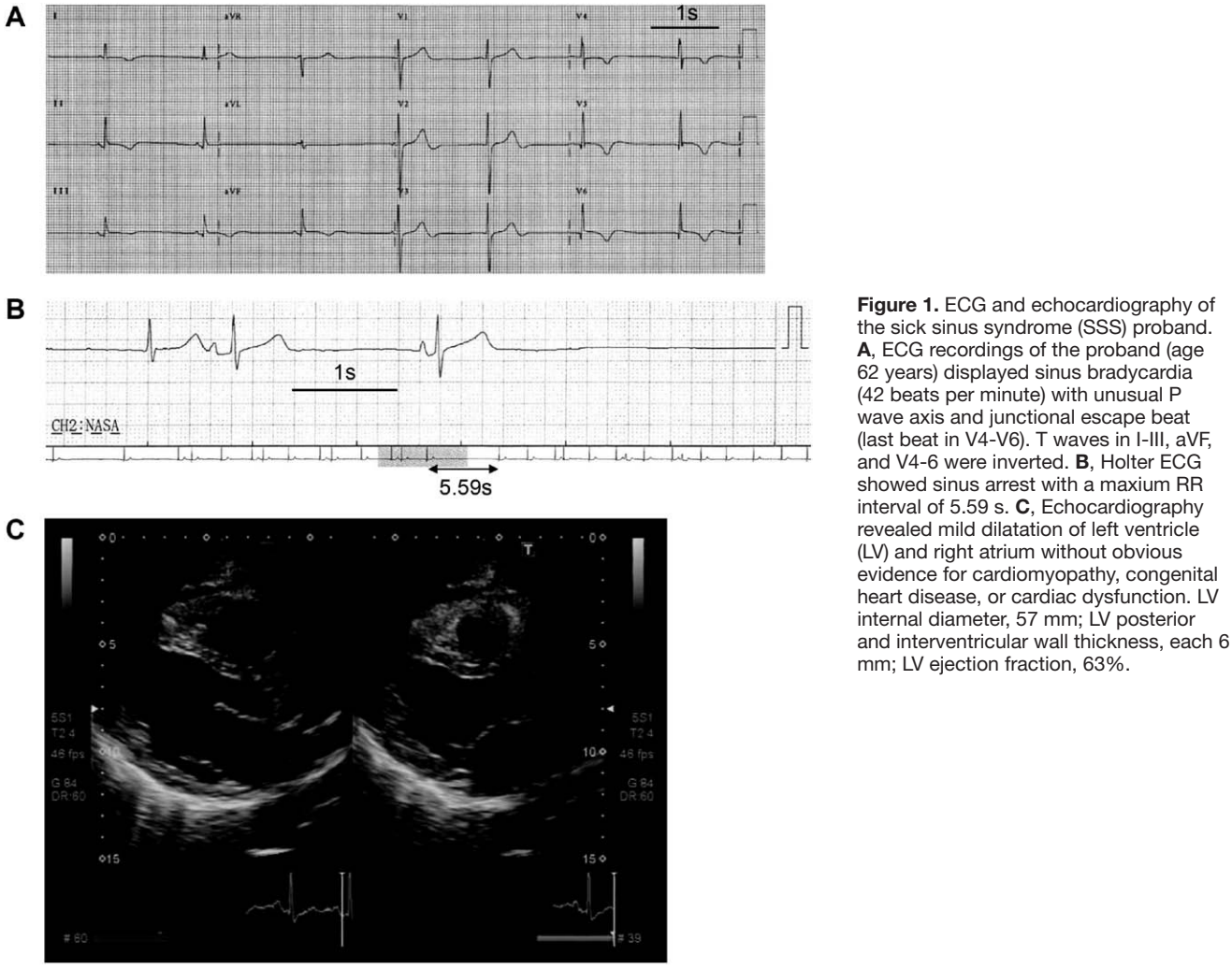

Figure 1. ECG and echocardiography of the sick sinus syndrome (SSS) proband. **A**, ECG recordings of the proband (age 62 years) displayed sinus bradycardia (42 beats per minute) with unusual P wave axis and junctional escape beat (last beat in V4-V6). T waves in I-III, aVF, and V4-6 were inverted. **B**, Holter ECG showed sinus arrest with a maxium RR interval of 5.59 s. **C**, Echocardiography revealed mild dilatation of left ventricle (LV) and right atrium without obvious evidence for cardiomyopathy, congenital heart disease, or cardiac dysfunction. LV internal diameter, 57 mm; LV posterior and interventricular wall thickness, each 6 mm; LV ejection fraction, 63%.

fluorescent microscopy at 48 hour-post-fertilization (hpf). Heart rate and rhythm were recorded. Videos obtained from the embryos were analyzed using Image J (National Institutes of Health) to determine the heart rate and the duration of cardiac pauses.

Statistical Analyses

Results are presented as means±SE otherwise stated, and statistical comparisons were made by using 1-way analysis of variance followed by Bonferroni adjustment to estimate the significance of differences between the mean values of all pairwise. Statistical significance was assumed for $P<0.05$.

Results

Case Presentation

Genetic screening of *MYH6* mutations in 9 probands with familial SSS identified a novel mutation in a 62-year-old Japanese woman. She attended the hospital because of several episodes of presyncope with which she had been afflicted for 5 years. Her 12-lead ECG showed sinus bradycardia (heart rate 42 beats per minute) with unusual P wave axis and junctional escape beat (Figure 1A), and Holter ECG revealed sinus arrest with maximum RR interval of 5.59 s (Figure 1B). She had no history of other arrhythmias, including atrial fibrillation. Echocardiography revealed mild dilatation of the left ventricle (LV) and right atrium, but there were no obvious signs of cardiomyopathy, congenital heart disease, or cardiac dysfunction (LV internal diameter in diastole, 57 mm; LV posterior wall in diastole, 6 mm; interventricular septal wall in diastole, 6 mm; and LV ejection fraction, 63%; Figure 1C). A pacemaker was implanted after the diagnosis of SSS. Her deceased mother also had a pacemaker implanted because of SSS during the 7th decade of her life.

Identification of the Novel *MYH6* Mutation delE933

The novel mutation identified in the proband was an in-frame 3-bp deletion, c.2797_2799delGAG, located in exon 22 of *MYH6*. This was predicted to delete one residue within the glutamic acid triplet at aa.931–933 of α-MHC (delE933; Figure 2A). This triplet is located in the S2 segment of α-MHC, a crucial structure required for binding to MyBP-C and for regional phosphorylation of MyBP-C,[6] thereby facilitating a flexible link between thin and thick filaments. The S2 hinge region is highly conserved among α-MHC from different species, as well as between other MHC isoforms (Figure 2B).

The proband has no siblings or offspring, and DNA was not available from her deceased mother. The delE933 mutation was not identified in 800 *MYH6* alleles from healthy Japanese controls or in the public genetic variation databases of dbSNP, 1000 Genomes, Exome Variant Server, and HGVD. The common variation A1101V was not found in the proband, whereas 3 out of 8 other probands in our cohort were heterozygous for A1101V. The rare *MYH6* variation R721W (c.C2161T), associated with SSS in Icelanders,[20] was not found in our familial SSS cohort. No other disease-related mutations were identified in *SCN5A*, *HCN4*, *SCN3B*, *KCNJ3*, *KCNJ5*, or *GJA5* in our familial SSS cohort. Polymorphisms identified in *MYH6* are listed in Table IV in the Data Supplement.

delE933-*MYH6* Mutation Disrupts Sarcomere Structures

The S2 segment is a coiled-coil domain of α-MHC composed of a motif of heptad repeats of amino acids.[6,29,30] SWISS-MODEL simulation predicted that the delE933 mutation would cause local disruption of the coiled-coil structure (Figure 3A). Immunoprecipitation studies using a recombinant MyBP-C C1-C2 protein and WT and delE933α-MHC S2 region proteins expressed in HeLa cells showed that the binding ability of α-MHC with MyBP-C was substantially enhanced by the delE933 mutation (Figure 3B).

Because structural damage of sarcomere have been reported in association with *MYH6* mutations responsible for atrial

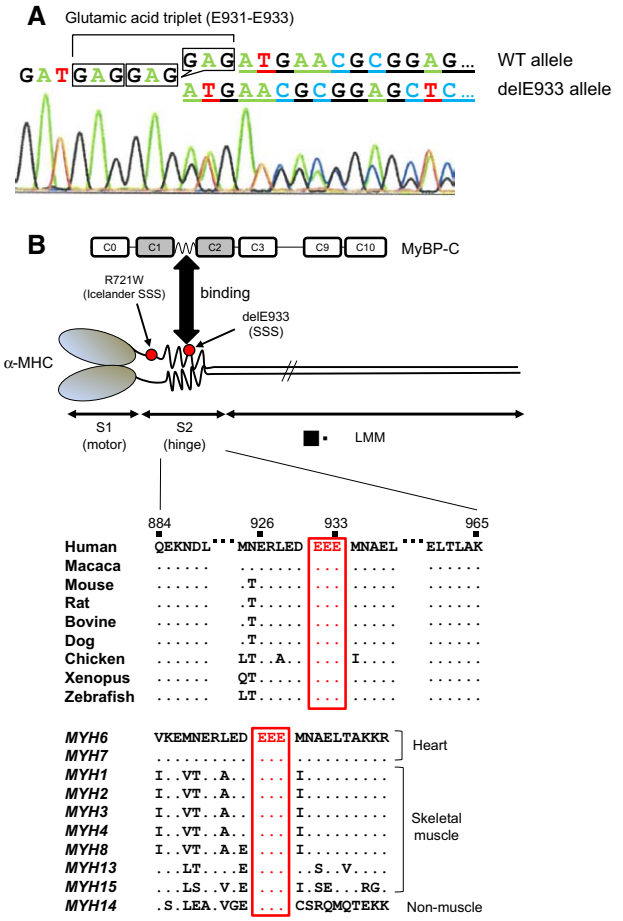

Figure 2. Genetic and protein information of the *MYH6* mutations. **A**, An electropherogram of exon 22 of *MYH6* of the proband. Boxes indicate the codons of triplicate glutamic acids E931-E933 of the wild-type (WT) allele and an in-frame deletion of GAG resulting in delE933. **B**, Protein structures of α-myosin heavy chain (α-MHC) and its binding partner myosin-binding protein C (MyBP-C). α-MHC consists of S1 motor, S2 hinge, and light meromyosin (LMM) regions. The S2 hinge region interacts with the region of MyBP-C between the 1st (C1) and 2nd globular structure (C2). Locations of the 2 *MYH6* mutations, a rare variant R721W identified in Icelanders[20] and delE933 (this study), are shown with red dots. Protein sequence alignment shows that the MyBP-C binding site (residues 884–965) are highly conserved among α-MHCs from different species, and the glutamic acid triplet is perfectly conserved among different species and different MHC isoforms of cardiac (*MYH6*, *MYH7*), skeletal muscle (*MYH1*, *MYH2*, *MYH3*, *MYH4*, *MYH8*, *MYH13*, *MYH15*), and a nonmuscle type (*MYH14*). SSS indicates sick sinus syndrome.

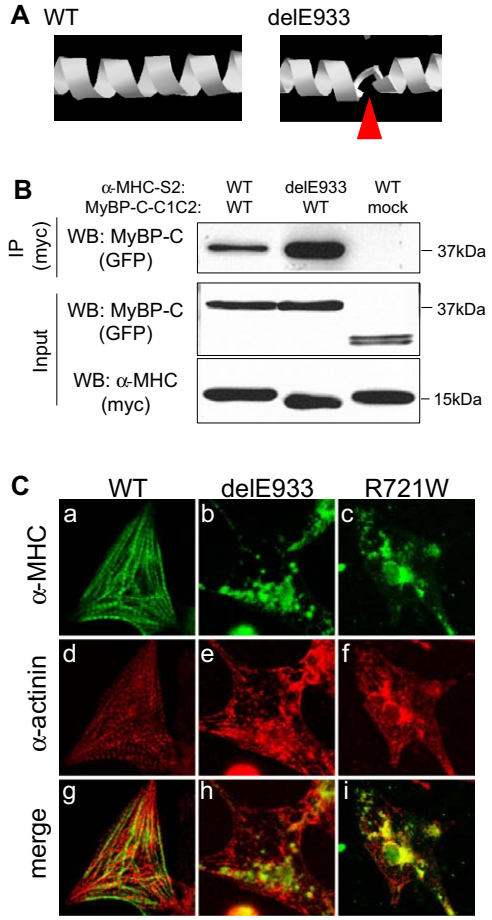

Figure 3. In silico prediction and in vitro functional evaluation of delE933-*MYH6*. **A**, Ribbon representation of 3-dimensional structure of the S2 region in human α-myosin heavy chain (α-MHC) predicted and visualized by SWISS-MODEL and RasTop, respectively. The coiled-coil structure is partially disrupted at the truncated amino acid E933 (arrowhead). **B**, Co-immunoprecipitation study of the S2 region of α-MHC and C1C2 region of cardiac myosin-binding protein C (MyBP-C). The S2 fragment of delE933 shows increased binding to the C1C2 fragment of MyBP-C. A nonspecific double band was often observed on the input of a mock pEGFP-C1 plasmid (third column). **C**, Fluorescence images of neonatal rat ventricular cardiomyocytes transiently expressing wild-type (WT), delE933, or R721W *MYH6* fused to green fluorescent protein (GFP). WT α-MHC shows a striated pattern of GFP together with the proper striated sarcomeric pattern of α-actinin (**a** and **d**). α-MHC with mutations of R721W and delE933 show brightly fluorescent speckles without well-organized sarcomere structure (**b** and **c**). The α-actinin images show a misaligned and disrupted pattern of myofibrils (**e** and **f**), indicating sarcomere disintegration. Scale bar, 10 μm.

septal defect,[7] we next explored whether the *MYH6* variation R721W, as well as delE933, disrupted integrity of sarcomere structures. To investigate the functional consequences of *MYH6* mutations on the atrial sarcomere structure, we used a heterologous expression system in cultured rat cardiomyocytes in which the predominant ventricle MHC isoform is α-MHC.[31] Neonatal rat ventricular cardiomyocytes were transiently transfected with a GFP-tagged *MYH6* WT, delE933, or R721W plasmids. Confocal microscopy analysis revealed comparable GFP intensities after transfection of all 3 *MYH6* plasmids (Figure 3C, a–c), indicating that the expression levels and stability of heterologously expressed α-MHC proteins were similar. Endogenous sarcomeric α-actinin expression at the Z-disc indicated the sarcomere integrity of transfected myocardial cells (Figure 3C, d–f). Cells expressing WT-*MYH6* displayed a striated staining pattern, indicating that heterologous α-MHC was correctly integrated into the sarcomere. However, both *MYH6* mutants, delE933 and R721W, exhibited a substantially disrupted α-actinin staining pattern and perinuclear aggregation of α-MHC, suggesting that structural damage to the sarcomere had occurred in cells expressing *MYH6* variants predisposing to sinus node dysfunction.

Atrial HL-1 Cells Stably Expressing the delE933-*MYH6* Showed Impaired Electric Propagation

A recent genome-wide association study showed that the Iceland-specific *MYH6* variant was significantly associated with atrial fibrillation,[20] we hypothesized that the functional defects caused by mutated *MYH6* may affect action potential propagation in the atrium surrounding the sinus node, leading to SSS manifestation. We cultured the mouse atrial cardiomyocyte cell line HL-1 stably expressing WT or mutant *MYH6* on 64-well electrode arrays and analyzed electric propagation velocities (Figure 4A). The propagation velocity was unchanged between WT-*MYH6* and control mock-transfected cells, but cells expressing delE933-*MYH6* exhibited a significantly slower propagation velocity (control, 3.6±0.6 mm/s; WT, 3.8±1.2 mm/s; delE933, 2.9±0.8 mm/s; n=252 for each line, $P<0.001$ for WT versus delE933; Figure 4B). Cell numbers of each array were comparable ($P=0.49$; Table V in the Data Supplement). These data suggest that mutant *MYH6* delE933 impairs cell-to-cell action potential propagation in the atrial myocardium.

delE933-*MYH6* Failed to Rescue the Heart Rate Reduction in Zebrafish With Morpholino *myh6* Knockdown

To determine whether the human *MYH6* orthologue *myh6* could influence heart rate control in zebrafish, we performed targeted *myh6* knockdown experiments with ATG-MO. Zebrafish cardiac phenotypes, including heart rate and cardiac rhythm, were assessed at 48 hpf. The *myh6* morphants exhibited atrial dilatation (Figure 4C), which is consistent with a previous report using decreased functional *myh6* transcript.[27] *Myh6* morphants also showed a significantly slower heart rate than uninjected embryos (*myh6*-MO, 137.7±2.2 beats per minute, n=28; uninjected 150.2±1.6 beats per minute, n=25; $P<0.001$; Figure 4D). Cardiac asystole was not observed in uninjected embryos or morphants. As shown in Figure 4D, coinjection of WT human *MYH6* cRNA rescued the bradycardia (148.7±1.4 beats per minute, n=26; versus *myh6*-MO $P<0.001$), suggesting that the human *MYH6* compensated for the loss of the zebrafish orthologue. By contrast, human *MYH6* carrying the delE933 mutation failed to rescue the bradycardia (142.3±2.5 beats per minute, n=24). Human *MYH6* RNA was detected by reverse transcription-polymerase chain reaction in embryos at 24 and 48 hours after injection (Figure in the Data Supplement), suggesting that the delE933 mutation of *MYH6* is responsible for sinus node dysfunction.

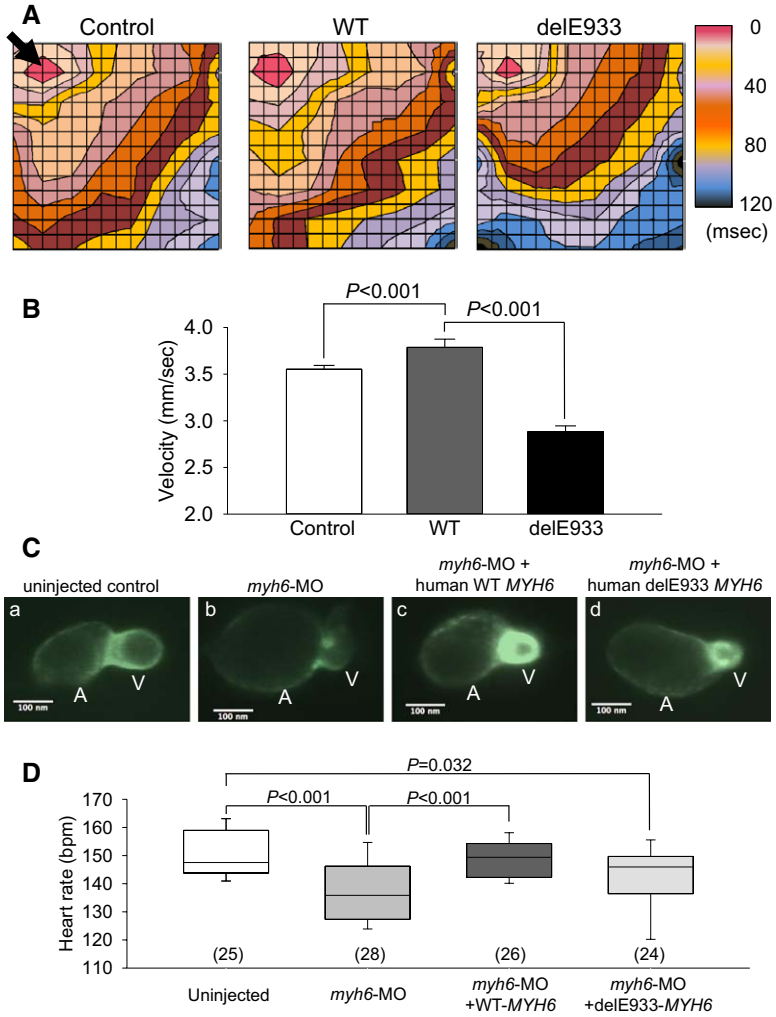

Figure 4. Electrophysiological phenotypes of delE933-*MYH6*. **A**, Representative activation isochronal maps of HL-1 cells stably expressing wild-type (WT) or delE933 *MYH6* and control HL-1 cells. An electric provocation with 10 μA was input on the pointed electrode (arrow). **B**, Averaged conduction velocity calculated from the time elapsed for the impulse to reach all remaining electrodes (n=252 for each recording). **C**, Representative fluorescent diastolic images of embryonic zebrafish hearts (atrium [A], ventricle [V]) at 48 hpf: uninjected control (**a**), *myh6*-MO only (**b**), *myh6*-MO coinjected with human WT *MYH6* cRNA (**c**), and *myh6*-MO coinjected with human delE933 *MYH6* cRNA (**d**). The atria of the *myh6* MO morphant in the presence or absence of coinjected human *MYH6* cRNAs (**b-d**) were slightly dilated compared with the uninjected control (**a**). The ventricle and cardiac looping pattern of the morphants, with or without *MYH6* cRNAs, were similar to that of the control. Scale bars, 100 μm **D**, Heart rate recordings from zebrafish (**a–d**). Data are shown as box and whisker plots with minimum, maximum, median, 25th, and 75th quartiles bars. Number in parentheses represents the number of zebrafish in each group.

Discussion

A growing body of evidence from genome-wide association studies has demonstrated an association of *MYH6* with sinus node function.[17–20] A common nonsynonymous single-nucleotide polymorphism of *MYH6* (A1101V) was previously shown to be a genetic modifier for resting heart rate and PR interval,[18] and this was further replicated in a large meta-analysis, including subjects of European ancestry from both the United States and Europe.[17,19] A combination of A1101V with other loci controlling heart rate further reduced the risk of SSS and pacemaker implantation, implicating a heritable quantitative trait.[17] By contrast, the rare *MYH6* variation R721W, unique to Icelanders, predisposes individuals to SSS and pacemaker implantation.[20] These studies clearly demonstrate that *MYH6* is a genetic modifier of sinus node function, but the mechanisms of this have been unclear, and it was uncertain whether *MYH6* could be a causative gene of familial SSS.

In this study, we identified a novel *MYH6* mutation, delE933, in one SSS individual among 9 probands of our familial SSS cohort.[22] We found that the mutant delE933-*MYH6* slowed down action potential propagation when heterologously expressed in the atrial myocardial cell line HL-1 (Figure 4A). Moreover, knockdown of endogenous *MYH6* leading to reduced heart rate in zebrafish could be compensated for by the coexpression of WT-*MYH6* but not by delE933-*MYH6* (Figure 4B). To our knowledge, this is the first experimental evidence demonstrating that *MYH6* variations can influence heart rate and action potential propagation. However, limited information is available to delineate the functional link between sarcomere components and sinus node function, and it remains unknown whether α-MHC directly affects pacemaker function or whether its actions are mediated though undefined mechanisms.

The delE933 mutation is located in the coiled-coil structure of the α-MHC S2 region, a binding motif for MyBP-C, and so is predicted to alter the tertiary structure and the cross-linking affinity between 2 sarcomere components (Figure 2A and 2B). Although the final consequences of such structural and functional modifications are unknown, a previous study that the MyBP-C mutation E334K, responsible for hypertrophic cardiomyopathy, impaired the ubiquitin-proteasome system, leading to an accumulation of cardiac ion channels at the sarcomere and electrophysiological dysfunction.[32] Increased protein levels were also observed for several other cardiac ion channels, including Kv1.5, Nav1.5, HCN4, Cav3.2, Cav1.2, SERCA, RYR2, and NCX1, which play major roles in controlling normal pacemaker function and atrial conductivity. Based on these findings, we speculate that an abnormal association

between delE933-α-MHC and MyBP-C might modulate the expression of cardiac ion channels that affect pacemaker function, which in turn would lead to the development of SSS.

In the present study, overexpression of the SSS-susceptible α-MHC mutants of R721W and delE933 in neonatal rat ventricular cardiomyocytes impaired sarcomere structures. However, it is unknown whether *MYH6* mutations preferentially impair the sinus node function or whether they might eventually cause further extensive electric damage manifesting as atrial fibrillation. Because the patient did not undergo electrophysiological studies or cardiac biopsy, further information regarding the spatial distribution and heterogeneity of pathological damages and electrophysiological abnormalities in the atrium is not available. Nevertheless, the T wave inversion of ECG and mild dilatation of the right atrium and LV (Figure 1A and 1B) are in accordance with the observation that targeted *myh6* knockdown in zebrafish induced the atrial dilatation associated with negative chronotropic effects, indicating that *MYH6* mutations may directly cause substantial damage and electric disorder to the myocardium in the atrium. This idea is further supported by the finding that heterozygous zebrafish expressing the *MYH6* mutation N695K (*MYH6*$^{hu/423/+}$) exhibited loss of atrial contractility, with residual beating restricted to the region near the atrioventricular junction and sinus venosus.[21] These observations strongly suggest that the final consequences of *MYH6* mutations in humans might also exhibit considerable heterogeneity with respect to the structural and electrophysiological properties of the atrium and sinus node.[33,34] Furthermore, these structural abnormalities of atrial sarcomere may extend to more severe conduction dysfunctions, such as atrial fibrillation or contractile failure, depending on the functional severity caused by each mutation. The slower conduction velocity observed in the HL-1 cells stably expressing delE933-*MYH6* in the present study suggests the possible involvement of *MYH6* in conduction dysfunction. This idea is supported by a recent genome-wide association study in which correlation studies of the *MYH6* variant R721W exhibited a significantly higher association with atrial fibrillation both before (odds ratio, 2.39; *P*=0.00010) and after (odds ratio, 2.03; *P*=0.015) exclusion of known SSS cases.[20] It is of note that the R719W of the ventricular β-MHC gene *MYH7*, homologous to the R721W-*MYH6,* is responsible for a malignant hypertrophic cardiomyopathy frequently associated with conduction abnormalities,[35] suggesting that α-MHC and β-MHC may share some pathophysiological mechanisms affecting cardiac action potential propagation.

SSS commonly occurs in older individual in the absence of accompanying heart diseases but comprises a variety of electrophysiological abnormalities in sinus node impulse formation and propagation. Although less common, SSS also shows familial inheritance, and implicated causative genes include those encoding cardiac ion channels, such as *SCN5A*. We recently found that familial SSS probands carrying *SCN5A* mutations showed a significantly earlier disease onset and a strong male predominance, whereas nonfamilial SSS had a disease onset of over 70 years for both sexes, which were affected equally.[22] The affected members of the SSS family in the present study were both women, aged over 60 years, suggesting that familial SSS with *MYH6* mutations might constitute an SSS subgroup distinct from that caused by *SCN5A* mutations. This may suggest the existence of a new disease entity of inherited arrhythmias attributable to mutations in genes encoding sarcomere proteins other than cardiac ion channel or ion channel-associated genes.

Limitation of the Study

Lack of information about the genotype–phenotype cosegregation of delE933-*MYH6* is the major limitation of this study from the standpoint of human genetics. Although bioinformatics evaluations, as well as in vitro and in vivo studies, have suggested pathophysiological significance of the rare *MYH6* variation delE933, it still does not exclude the possibility that the proband manifested SSS attributable to factors, such as aging rather than the *MYH6* mutation. To demonstrate the causality between SSS and *MYH6*, more extensive genetic screenings in patients with familial SSS to find novel *MYH6* mutations are required. Furthermore, it remains to be elucidated how the impaired sarcomere structures and conduction velocity elicited by delE933-*MYH6* ultimately result in the sinus node dysfunction. Electrophysiological studies using induced pluripotent stem cell–derived cardiomyocytes from *MYH6* mutation carriers, as well as basic evaluations of *MYH6* using genetically engineered animals, are also warranted.

Acknowledgments

We are indebted to Saori Nakano, Atsuko Iida, and Yasuko Noguchi for technical assistance and attending physicians for referring SSS patients.

Sources of Funding

This work was supported by Grant-in-Aid for Scientific Research on Innovative Areas (HD Physiology) 22136007 (N. Makita) and Grants-in-Aid for Scientific Research 26860572 (T. Ishikawa), 24390199 (N. Makita), 25293181 and 25670172 (A. Kimura) from the Ministry of Education, Culture, Sports, Science and Technology, Japan; Research Grant for the Cardiovascular Diseases (H24-033) from the Japanese Ministry of Health, Labour and Welfare (N. Makita); the Joint Usage/Research Program of Medical Research Institute Tokyo Medical and Dental University (N. Makita, A.K.); a research grant from Fukuda Foundation for Medical Technology (T. Ishikawa); Joint Research Promotion Project of Nagasaki University Graduate School of Biomedical Sciences (T. Ishikawa); and Fellow-to Faculty Award from American Heart Association (C.J. Jou).

Disclosures

None.

References

1. Mangrum JM, DiMarco JP. The evaluation and management of bradycardia. *N Engl J Med*. 2000;342:703–709. doi: 10.1056/NEJM200003093421006.
2. Benson DW, Wang DW, Dyment M, Knilans TK, Fish FA, Strieper MJ, Rhodes TH, George AL Jr. Congenital sick sinus syndrome caused by recessive mutations in the cardiac sodium channel gene (SCN5A). *J Clin Invest*. 2003;112:1019–1028. doi: 10.1172/JCI18062.
3. Mohler PJ, Splawski I, Napolitano C, Bottelli G, Sharpe L, Timothy K, Priori SG, Keating MT, Bennett V. A cardiac arrhythmia syndrome caused by loss of ankyrin-B function. *Proc Natl Acad Sci U S A*. 2004;101:9137–9142. doi: 10.1073/pnas.0402546101.
4. Nof E, Luria D, Brass D, Marek D, Lahat H, Reznik-Wolf H, Pras E, Dascal N, Eldar M, Glikson M. Point mutation in the HCN4 cardiac ion

channel pore affecting synthesis, trafficking, and functional expression is associated with familial asymptomatic sinus bradycardia. *Circulation*. 2007;116:463–470. doi: 10.1161/CIRCULATIONAHA.107.706887.
5. Amin AS, Asghari-Roodsari A, Tan HL. Cardiac sodium channelopathies. *Pflugers Arch*. 2010;460:223–237. doi: 10.1007/s00424-009-0761-0.
6. Harris SP, Rostkova E, Gautel M, Moss RL. Binding of myosin binding protein-C to myosin subfragment S2 affects contractility independent of a tether mechanism. *Circ Res*. 2004;95:930–936. doi: 10.1161/01.RES.0000147312.02673.56.
7. Granados-Riveron JT, Ghosh TK, Pope M, Bu'Lock F, Thornborough C, Eason J, Kirk EP, Fatkin D, Feneley MP, Harvey RP, Armour JA, David Brook J. Alpha-cardiac myosin heavy chain (MYH6) mutations affecting myofibril formation are associated with congenital heart defects. *Hum Mol Genet*. 2010;19:4007–4016. doi: 10.1093/hmg/ddq315.
8. Gruen M, Gautel M. Mutations in beta-myosin S2 that cause familial hypertrophic cardiomyopathy (FHC) abolish the interaction with the regulatory domain of myosin-binding protein-C. *J Mol Biol*. 1999;286:933–949. doi: 10.1006/jmbi.1998.2522.
9. Reiser PJ, Kline WO. Electrophoretic separation and quantitation of cardiac myosin heavy chain isoforms in eight mammalian species. *Am J Physiol*. 1998;274(3 Pt 2):H1048–H1053.
10. Kimura A. Molecular etiology and pathogenesis of hereditary cardiomyopathy. *Circ J*. 2008;72 Suppl A:A38–A48.
11. Lakdawala NK, Winterfield JR, Funke BH. Dilated cardiomyopathy. *Circ Arrhythm Electrophysiol*. 2013;6:228–237. doi: 10.1161/CIRCEP.111.962050.
12. Carniel E, Taylor MR, Sinagra G, Di Lenarda A, Ku L, Fain PR, Boucek MM, Cavanaugh J, Miocic S, Slavov D, Graw SL, Feiger J, Zhu XZ, Dao D, Ferguson DA, Bristow MR, Mestroni L. Alpha-myosin heavy chain: a sarcomeric gene associated with dilated and hypertrophic phenotypes of cardiomyopathy. *Circulation*. 2005;112:54–59. doi: 10.1161/CIRCULATIONAHA.104.507699.
13. Niimura H, Patton KK, McKenna WJ, Soults J, Maron BJ, Seidman JG, Seidman CE. Sarcomere protein gene mutations in hypertrophic cardiomyopathy of the elderly. *Circulation*. 2002;105:446–451.
14. Ching YH, Ghosh TK, Cross SJ, Packham EA, Honeyman L, Loughna S, Robinson TE, Dearlove AM, Ribas G, Bonser AJ, Thomas NR, Scotter AJ, Caves LS, Tyrrell GP, Newbury-Ecob RA, Munnich A, Bonnet D, Brook JD. Mutation in myosin heavy chain 6 causes atrial septal defect. *Nat Genet*. 2005;37:423–428. doi: 10.1038/ng1526.
15. Posch MG, Waldmuller S, Müller M, Scheffold T, Fournier D, Andrade-Navarro MA, De Geeter B, Guillaumont S, Dauphin C, Yousseff D, Schmitt KR, Perrot A, Berger F, Hetzer R, Bouvagnet P, Özcelik C. Cardiac alpha-myosin (MYH6) is the predominant sarcomeric disease gene for familial atrial septal defects. *PLoS One*. 2011;6:e28872. doi: 10.1371/journal.pone.0028872.
16. Arrington CB, Bleyl SB, Matsunami N, Bonnell GD, Otterud BE, Nielsen DC, Stevens J, Levy S, Leppert MF, Bowles NE. Exome analysis of a family with pleiotropic congenital heart disease. *Circ Cardiovasc Genet*. 2012;5:175–182. doi: 10.1161/CIRCGENETICS.111.961797.
17. den Hoed M, Eijgelsheim M, Esko T, Brundel BJ, Peal DS, Evans DM, Nolte IM, Segrè AV, Holm H, Handsaker RE, Westra HJ, Johnson T, Isaacs A, Yang J, Lundby A, Zhao JH, Kim YJ, Go MJ, Almgren P, Bochud M, Boucher G, Cornelis MC, Gudbjartsson D, Hadley D, van der Harst P, Hayward C, den Heijer M, Igl W, Jackson AU, Kutalik Z, Luan J, Kemp JP, Kristiansson K, Ladenvall C, Lorentzon M, Montasser ME, Njajou OT, O'Reilly PF, Padmanabhan S, St Pourcain B, Rankinen T, Salo P, Tanaka T, Timpson NJ, Vitart V, Waite L, Wheeler W, Zhang W, Draisma HH, Feitosa MF, Kerr KF, Lind PA, Mihailov E, Onland-Moret NC, Song C, Weedon MN, Xie W, Yengo L, Absher D, Albert CM, Alonso A, Arking DE, de Bakker PI, Balkau B, Barlassina C, Benaglio P, Bis JC, Bouatia-Naji N, Brage S, Chanock SJ, Chines PS, Chung M, Darbar D, Dina C, Dörr M, Elliott P, Felix SB, Fischer K, Fuchsberger C, de Geus EJ, Goyette P, Gudnason V, Harris TB, Hartikainen AL, Havulinna AS, Heckbert SR, Hicks AA, Hofman A, Holewijn S, Hoogstra-Berends F, Hottenga JJ, Jensen MK, Johansson A, Junttila J, Kääb S, Kanon B, Ketkar S, Khaw KT, Knowles JW, Kooner AS, Kors JA, Kumari M, Milani L, Laiho P, Lakatta EG, Langenberg C, Leusink M, Liu Y, Luben RN, Lunetta KL, Lynch SN, Markus MR, Marques-Vidal P, Mateo Leach I, McArdle WL, McCarroll SA, Medland SE, Miller KA, Montgomery GW, Morrison AC, Müller-Nurasyid M, Navarro P, Nelis M, O'Connell JR, O'Donnell CJ, Ong KK, Newman AB, Peters A, Polasek O, Pouta A, Pramstaller PP, Psaty BM, Rao DC, Ring SM, Rossin EJ, Rudan D, Sanna S, Scott RA, Sehmi JS, Sharp S, Shin JT, Singleton AB, Smith AV, Soranzo N, Spector TD, Stewart C, Stringham HM, Tarasov KV, Uitterlinden AG, Vandenput L, Hwang SJ, Whitfield JB, Wijmenga C, Wild SH, Willemsen G, Wilson JF, Witteman JC, Wong A, Wong Q, Jamshidi Y, Zitting P, Boer JM, Boomsma DI, Borecki IB, van Duijn CM, Ekelund U, Forouhi NG, Froguel P, Hingorani A, Ingelsson E, Kivimaki M, Kronmal RA, Kuh D, Lind L, Martin NG, Oostra BA, Pedersen NL, Quertermous T, Rotter JI, van der Schouw YT, Verschuren WM, Walker M, Albanes D, Arnar DO, Assimes TL, Bandinelli S, Boehnke M, de Boer RA, Bouchard C, Caulfield WL, Chambers JC, Curhan G, Cusi D, Eriksson J, Ferrucci L, van Gilst WH, Glorioso N, de Graaf J, Groop L, Gyllensten U, Hsueh WC, Hu FB, Huikuri HV, Hunter DJ, Iribarren C, Isomaa B, Jarvelin MR, Jula A, Kähönen M, Kiemeney LA, van der Klauw MM, Kooner JS, Kraft P, Iacoviello L, Lehtimäki T, Lokki ML, Mitchell BD, Navis G, Nieminen MS, Ohlsson C, Poulter NR, Qi L, Raitakari OT, Rimm EB, Rioux JD, Rizzi F, Rudan I, Salomaa V, Sever PS, Shields DC, Shuldiner AR, Sinisalo J, Stanton AV, Stolk RP, Strachan DP, Tardif JC, Thorsteinsdottir U, Tuomilehto J, van Veldhuisen DJ, Virtamo J, Viikari J, Vollenweider P, Waeber G, Widen E, Cho YS, Olsen JV, Visscher PM, Willer C, Franke L, Erdmann J, Thompson JR, Pfeufer A, Sotoodehnia N, Newton-Cheh C, Ellinor PT, Stricker BH, Metspalu A, Perola M, Beckmann JS, Smith GD, Stefansson K, Wareham NJ, Munroe PB, Sibon OC, Milan DJ, Snieder H, Samani NJ, Loos RJ; Global BPgen Consortium; CARDIoGRAM Consortium; PR GWAS Consortium; QRS GWAS Consortium; QT-IGC Consortium; CHARGE-AF Consortium. Identification of heart rate-associated loci and their effects on cardiac conduction and rhythm disorders. *Nat Genet*. 2013;45:621–631. doi: 10.1038/ng.2610.
18. Holm H, Gudbjartsson DF, Arnar DO, Thorleifsson G, Thorgeirsson G, Stefansdottir H, Gudjonsson SA, Jonasdottir A, Mathiesen EB, Njølstad I, Nyrnes A, Wilsgaard T, Hald EM, Hveem K, Stoltenberg C, Løchen ML, Kong A, Thorsteinsdottir U, Stefansson K. Several common variants modulate heart rate, PR interval and QRS duration. *Nat Genet*. 2010;42:117–122. doi: 10.1038/ng.511.
19. Eijgelsheim M, Newton-Cheh C, Sotoodehnia N, de Bakker PI, Müller M, Morrison AC, Smith AV, Isaacs A, Sanna S, Dörr M, Navarro P, Fuchsberger C, Nolte IM, de Geus EJ, Estrada K, Hwang SJ, Bis JC, Rückert IM, Alonso A, Launer LJ, Hottenga JJ, Rivadeneira F, Noseworthy PA, Rice KM, Perz S, Arking DE, Spector TD, Kors JA, Aulchenko YS, Tarasov KV, Homuth G, Wild SH, Marroni F, Gieger C, Licht CM, Prineas RJ, Hofman A, Rotter JI, Hicks AA, Ernst F, Najjar SS, Wright AF, Peters A, Fox ER, Oostra BA, Kroemer HK, Couper D, Völzke H, Campbell H, Meitinger T, Uda M, Witteman JC, Psaty BM, Wichmann HE, Harris TB, Kääb S, Siscovick DS, Jamshidi Y, Uitterlinden AG, Folsom AR, Larson MG, Wilson JF, Penninx BW, Snieder H, Pramstaller PP, van Duijn CM, Lakatta EG, Felix SB, Gudnason V, Pfeufer A, Heckbert SR, Stricker BH, Boerwinkle E, O'Donnell CJ. Genome-wide association analysis identifies multiple loci related to resting heart rate. *Hum Mol Genet*. 2010;19:3885–3894. doi: 10.1093/hmg/ddq303.
20. Holm H, Gudbjartsson DF, Sulem P, Masson G, Helgadottir HT, Zanon C, Magnusson OT, Helgason A, Saemundsdottir J, Gylfason A, Stefansdottir H, Gretarsdottir S, Matthiasson SE, Thorgeirsson GM, Jonasdottir A, Sigurdsson A, Stefansson H, Werge T, Rafnar T, Kiemeney LA, Parvez B, Muhammad R, Roden DM, Darbar D, Thorleifsson G, Walters GB, Kong A, Thorsteinsdottir U, Arnar DO, Stefansson K. A rare variant in MYH6 is associated with high risk of sick sinus syndrome. *Nat Genet*. 2011;43:316–320. doi: 10.1038/ng.781.
21. Singleman C, Holtzman NG. Analysis of postembryonic heart development and maturation in the zebrafish, Danio rerio. *Dev Dyn*. 2012;241:1993–2004. doi: 10.1002/dvdy.23882.
22. Abe K, Machida T, Sumitomo N, Yamamoto H, Ohkubo K, Watanabe I, Makiyama T, Fukae S, Kohno M, Harrell DT, Ishikawa T, Tsuji Y, Nogami A, Watabe T, Oginosawa Y, Abe H, Maemura K, Motomura H, Makita N. Sodium channelopathy underlying familial sick sinus syndrome with early onset and predominantly male characteristics. *Circ Arrhythm Electrophysiol*. 2014;7:511–517. doi: 10.1161/CIRCEP.113.001340.
23. Turner DL, Weintraub H. Expression of achaete-scute homolog 3 in Xenopus embryos converts ectodermal cells to a neural fate. *Genes Dev*. 1994;8:1434–1447.
24. Rupp RA, Snider L, Weintraub H. Xenopus embryos regulate the nuclear localization of XMyoD. *Genes Dev*. 1994;8:1311–1323.
25. Arimura T, Ishikawa T, Nunoda S, Kawai S, Kimura A. Dilated cardiomyopathy-associated BAG3 mutations impair Z-disc assembly and enhance sensitivity to apoptosis in cardiomyocytes. *Hum Mutat*. 2011;32:1481–1491. doi: 10.1002/humu.21603.
26. White SM, Constantin PE, Claycomb WC. Cardiac physiology at the cellular level: use of cultured HL-1 cardiomyocytes for studies of cardiac muscle cell structure and function. *Am J Physiol Heart Circ Physiol*. 2004;286:H823–H829. doi: 10.1152/ajpheart.00986.2003.

27. Berdougo E, Coleman H, Lee DH, Stainier DY, Yelon D. Mutation of weak atrium/atrial myosin heavy chain disrupts atrial function and influences ventricular morphogenesis in zebrafish. *Development*. 2003;130:6121–6129. doi: 10.1242/dev.00838.
28. Kimmel CB, Ballard WW, Kimmel SR, Ullmann B, Schilling TF. Stages of embryonic development of the zebrafish. *Dev Dyn*. 1995;203:253–310. doi: 10.1002/aja.1002030302.
29. Kunst G, Kress KR, Gruen M, Uttenweiler D, Gautel M, Fink RH. Myosin binding protein C, a phosphorylation-dependent force regulator in muscle that controls the attachment of myosin heads by its interaction with myosin S2. *Circ Res*. 2000;86:51–58.
30. Palmer BM, Georgakopoulos D, Janssen PM, Wang Y, Alpert NR, Belardi DF, Harris SP, Moss RL, Burgon PG, Seidman CE, Seidman JG, Maughan DW, Kass DA. Role of cardiac myosin binding protein C in sustaining left ventricular systolic stiffening. *Circ Res*. 2004;94:1249–1255. doi: 10.1161/01.RES.0000126898.95550.31.
31. Hughes SE, McKenna WJ. New insights into the pathology of inherited cardiomyopathy. *Heart*. 2005;91:257–264. doi: 10.1136/hrt.2004.040337.
32. Bahrudin U, Morikawa K, Takeuchi A, Kurata Y, Miake J, Mizuta E, Adachi K, Higaki K, Yamamoto Y, Shirayoshi Y, Yoshida A, Kato M, Yamamoto K, Nanba E, Morisaki H, Morisaki T, Matsuoka S, Ninomiya H, Hisatome I. Impairment of ubiquitin-proteasome system by E334K cMyBPC modifies channel proteins, leading to electrophysiological dysfunction. *J Mol Biol*. 2011;413:857–878. doi: 10.1016/j.jmb.2011.09.006.
33. Chandler NJ, Greener ID, Tellez JO, Inada S, Musa H, Molenaar P, Difrancesco D, Baruscotti M, Longhi R, Anderson RH, Billeter R, Sharma V, Sigg DC, Boyett MR, Dobrzynski H. Molecular architecture of the human sinus node: insights into the function of the cardiac pacemaker. *Circulation*. 2009;119:1562–1575. doi: 10.1161/CIRCULATIONAHA.108.804369.
34. Yamamoto M, Dobrzynski H, Tellez J, Niwa R, Billeter R, Honjo H, Kodama I, Boyett MR. Extended atrial conduction system characterised by the expression of the HCN4 channel and connexin45. *Cardiovasc Res*. 2006;72:271–281. doi: 10.1016/j.cardiores.2006.07.026.
35. Anan R, Greve G, Thierfelder L, Watkins H, McKenna WJ, Solomon S, Vecchio C, Shono H, Nakao S, Tanaka H. Prognostic implications of novel beta cardiac myosin heavy chain gene mutations that cause familial hypertrophic cardiomyopathy. *J Clin Invest*. 1994;93:280–285. doi: 10.1172/JCI116957.

SUPPLEMENTAL MATERIALS

Supplemental Method

Detection of the injected human *MYH6* cRNA in zebrafish embryos

Myh6 ATG-MO (0.5-1 ng/embryo) was co-injected with WT or delE933 *MYH6* cRNA (0.4 ng/embryo) at the 1- to 2-cell stage. After the injection, embryos were collected at 24 and 48 hpf. The uninjected embryos were collected at 48 hpf. To validate the expression of the exogenously injected human *MYH6* cRNAs in the embryonic bodies, total RNA was extracted from whole embryo using protocol based on QIAGEN RNeasy Mini Kit (Qiagen, Venlo, Netherlands). cDNA libraries were constructed by reverse transcriptase-PCR (RT-PCR) using the Ambion RETROscript Kit (Life Technologies). PCR was performed using *MYH6* primers (MYH6-2555F and MYH6-2935R; Supplemental Table S1) designed to specifically amplify human *MYH6* (402 bp) but not intrinsic zebrafish *myh6*. An aliquot of PCR product was loaded on an agarose gel, and then sequenced using ABI 3130 genetic analyzer (Life Technologies).

Supplemental Result

Expression of the injected human *MYH6* cRNA in zebrafish embryos

As shown in the supplemental figure, primer set of MYH6-2555F and MYH6-2935R successfully amplified a single human *MYH6* fragment (402 bp, arrowhead) from whole zebrafish embryos (lane 2, 3: co-injected with myh6 ATG-MO and WT-*MYH6* cRNA; lane 4, 5: co-injected with myh6 ATG-MO and delE933-*MYH6* cRNA) both at 24 and 48 hpf, but not from uninjected embryo (Ct). WT and delE933 human *MYH6* sequences of the PCR products were confirmed (not shown). These data support that the inability of delE933 to rescue heart rate suppression by myh6 ATG-MO is attributable to the properties of overexpressed delE933-*MYH6*, rather than technical inadequacy such as RNA degradation.

Supplemental Figure

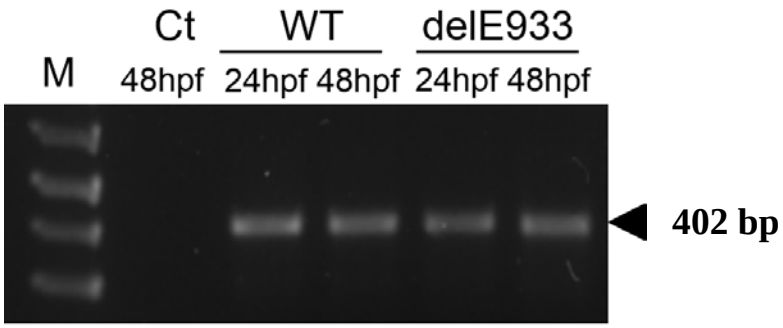

RT-PCR shows the presence of human *MYH6* RNAs in zebrafish embryos at 24h and 48h after co-injection of myh6 ATG-morpholino and *MYH6* cRNA of either WT or delE933. Primers were designed to specifically amplify a 402 bp fragment (arrowhead) of human *MYH6*, but not zebrafish *myh6*. Ct: Control (uninjected embryos), M: 100 bp marker

Table S1. Nucleotide sequences of the primers

1. Genetic screening of *MYH6*

Analyzed region	Forward primer (5’ to 3’)	Reverse primer (5’ to 3’)
Exon 3	AGAGGACAAAGCCACTCGCTG	TGCAAGTGGCTCCACCTCTG
Exons 4-6	AATGGGAAGGGAAATTACCTG	CTAGGCATCAGCGTGTCTGC
Exons 7-8	CCCTGTATGGAGAACAGTAG	TGGGTGTGGCAAAACAGCAC
Exons 9-10	CATTTCCAGAACCATCCAGG	CCTGCATGCAGGAGTCGTTG
Exons 11-12	TTGCCTGGTGCAGACATGCTG	AGAGAGCCTGGTCAGCACCTC
Exon 13	GTGCTCACTTATCCTTTCCC	CTCTCAGCAAATGGCTGTTG
Exon 14	CAACAGCCATTTGCTGAGAG	CTCTAGTTTCTTGGGTGTAG
Exon 15	TGTCAGGGTATGGGACTGTG	GTGCTTTGAAGCAGCAGGAC
Exons 16-20	AAAGTCTCAGAGCTACCAAGCG	CTTCTGACCCACACTAGTTGAC
Exons 21-23	AGTCTACGTGCCTACGAACTTG	CAGGACTTTCTGGGCCATTGG
Exons 24-25	GAAGGAGGCAAAAGAGCATAC	CTGCAGCCTCAGTTACCTCAG
Exons 26-28	TTCCTGGTAGCTTTTCAGAGC	TCCATTTCTGGCACTGAGATG
Exons 29-30	AAGGCTGGGCTTGGTTGAAG	AGCCGCATGTCCAAGATCTG
Exons 31-32	CAGATCTTGGACATGCGGCT	AGATTTTGTCCTGGGGTCAG
Exons 33-34	ACCGTGTATCTTCTCATCCTC	ACTCAGTAGGTTTCCACAAGG
Exons 35-36	ACCACCTTTAATTCTTTCTGG	TAAATCTACCAACAGCATCTC
Exon 37	GGGAAAGGTGATTGCATTTGC	AGCAAACTCTTTGTCCAGGCC
Exon 38	GTTGCAGGAATATGCATGAGG	ACATATAGGGCAAGCAGTGCC
Exon 39	ACCACAAGTGCCTCTAACGTG	CTACTGCCCTGATCCAGGATG

2. Plasmid constructions of α-MHC and MyBP-C

Name	Sequence (5’ to 3’)
MYH6-F-EcoRV	TCCGGACTCAGATCGATATCAATGACCGATGCCCAGATGGCTG
MYH6-R-Sal1-N	GCGGTACCGTCGACGTGTCACTCCTCATCGTGCATTTTTTGC
MYH6-933del-A-RN	CCGCGTTCATCTCCTCATCCTCCAGCCTCTCATTCATC
MYH6-933del-P-FN	GGATGAGGAGATGAACGCGGAGCTCACTGCCAAGAAG
MYH6-R721W-A-R	CGGAAGTCCCCATAGAGGATGCGGTTG
MYH6-R721W-P-F	ATCCTCTATGGGGACTTCCGGCAGAGGTATC
MYH6-F-Cla1	TCCGGACTCAGATATCGATAAATGCACCATGCCCAG
MYH6-R-Xho1	TGGATCCCGGGCTCGAGGTACCGTCGACGTGTCACTC
MYH6-pIRES-Nhe1-F	CCGGACTCAGCTAGCCCACCATGACCGATGCCCAGATGGCTG
MYH6-pIRES-Sal1-R	TACCGTCGACGTGTCACTCCTCATCGTGCATTTTTTGCTTG
MYH6-S2-F-Bam	ACTTCAAGGATCCGCCGCTGCTGAAGAGCGCAGAG
MYH6-S2-R-Eco	TCTCCTTGAATTCCTTGGCCAGTGTCAGCTCCAG
MYBPC3-C1C2-F-Eco	CCCGGGCGAATTCTGTCCACGAGGCCATG
MYBPC3-C1C2-R-Sal	TTGATATCGTCGACTGTGCTCTTCTTCTC

3. RT-PCR of human *MYH6* in zebrafish embryos

Name	Sequence (5’ to 3’)
MYH6-2555F	CCACCATGAAGGAAGAGTTCG
MYH6-2935R	CAGCCATCTCCTCTGTTAGGTT

4. ATG-blocking morpholino antisense oligonucleotide targeting zebrafish *myh6*

Name	Sequence (5’ to 3’)
myh6 ATG-MO	ACTCTGCCATTAAAGCATCACCCAT

Table S2. GenBank accession numbers of human *MYH* paralogs

Genes	GenBank accession number
MYH1	NP_005954
MYH2	NP_060004
MYH3	NP_002461
MYH4	NP_060003
MYH6	NP_002462
MYH7	NP_000248
MYH8	NP_002463
MYH13	NP_003793
MYH14	NP_079005
MYH15	NP_055796

Table S3. GenBank accession numbers of α-MHC orthologs

Species	GenBank accession number
human	NP_002462
macaque	XP_001102827
mouse	NP_001157643
rat	NP_058935
bovine	XP_002690549
dog	XP_003435121
chicken	NP_990097
xenopus	NP_001085070
zebrafish	NP_942118

Table S4. *MYH6* exon variations in nine SSS probands

Exon	Nucleotide position	Changes of amino acid and nucleotide	Number of patients	dbSNP
17	2151	Y717Y (TAC to TAT)	1	rs76202964
22	2797-2799	delE933 (del_GAG)	1	-
25	3302	A1101V (GTG to GCG)	3	rs365990
32	4527	E1509E (GAG to GAA)	1	rs34855944
33	4777	Q1593L (CAG to CTG)	1	rs45574136
33	4838	V1613A (GTC to GCC)	4	rs61742476
33	4914	A1638A (GCT to GCC)	1	rs178640

Table S5. Cell counting on multi-electrode arrays

Line	Control pIRES2-EGFP	WT-*MYH6*	delE933-*MYH6*
1	2.45	2.12	2.34
2	2.00	2.55	2.11
3	2.91	2.13	2.23
4	2.56	2.38	2.41
			$x10^5$ cells

Novel Mutation in the α-Myosin Heavy Chain Gene Is Associated With Sick Sinus Syndrome

Taisuke Ishikawa, Chuanchau J. Jou, Akihiko Nogami, Shinya Kowase, Cammon B. Arrington, Spencer M. Barnett, Daniel T. Harrell, Takuro Arimura, Yukiomi Tsuji, Akinori Kimura and Naomasa Makita

Circ Arrhythm Electrophysiol. 2015;8:400-408; originally published online February 25, 2015;
doi: 10.1161/CIRCEP.114.002534
Circulation: Arrhythmia and Electrophysiology is published by the American Heart Association, 7272 Greenville Avenue, Dallas, TX 75231

Print ISSN: 1941-3149. Online ISSN: 1941-3084